Journal of
Materials Chemistry B

Accepted Manuscript

This article can be cited before page numbers have been issued, to do this please use: Z. Chen, D. chengtiewu@mail.sic.ac.cn Yi, X. Zheng, J. Chang, C. Wu and Y. Xiao, *J. Mater. Chem. B*, 2014, DOI: 10.1039/C4TB00837E.

This is an *Accepted Manuscript*, which has been through the Royal Society of Chemistry peer review process and has been accepted for publication.

Accepted Manuscripts are published online shortly after acceptance, before technical editing, formatting and proof reading. Using this free service, authors can make their results available to the community, in citable form, before we publish the edited article. We will replace this *Accepted Manuscript* with the edited and formatted *Advance Article* as soon as it is available.

You can find more information about *Accepted Manuscripts* in the Information for Authors.

Please note that technical editing may introduce minor changes to the text and/or graphics, which may alter content. The journal's standard Terms & Conditions and the Ethical guidelines still apply. In no event shall the Royal Society of Chemistry be held responsible for any errors or omissions in this *Accepted Manuscript* or any consequences arising from the use of any information it contains.

ROYAL SOCIETY OF CHEMISTRY

www.rsc.org/materialsB

View Article Online
DOI: 10.1039/C4TB00837E

Nutrient element-based bioceramic coatings on titanium alloy stimulating osteogenesis via inducing beneficial osteoimmmunomodulation

Zetao Chen [1, 2], Deliang Yi [3], Xuebin Zheng[4], Jiang Chang [2, 3], Chengtie Wu [2, 3]*, Yin Xiao [1, 2]*

1. Institute of Health and Biomedical Innovation, Queensland University of Technology, Brisbane, 60 Musk Ave, Kelvin Grove, Brisbane, Queensland 4059, Australia

2. Australia-China Centre for Tissue Engineering and Regenerative Medicine, Queensland University of Technology, Brisbane, 60 Musk Ave, Kelvin Grove, Brisbane, Queensland 4059, Australia

3. State Key Laboratory of High Performance Ceramics and Superfine Microstructure, Shanghai Institute of Ceramics, Chinese Academy of Sciences, 1295 Dingxi Road, Shanghai 200050, People's Republic of China

4. Key Laboratory of Inorganic Coating Materials, Chinese Academy of Science, 1295 Dingxi Road, Shanghai 200050, People's Republic of China

Z.C and D.Y are co-first authors.

*** Corresponding authors.**

Email: chengtiewu@mail.sic.ac.cn (C. Wu)

Tel: +86-21-52412249; Fax: +86-21-52413903.

E-mail: yin.xiao@qut.edu.au (Y. Xiao)

Tel.: +61 7 3138 6240; fax: +61 7 3138 6030.

View Article Online
DOI: 10.1039/C4TB00837E

ABSTRACT

A paradigm shift has taken place in which bone implant materials has gone from being relatively inert to having immunomodulatory properties, emphasizing the importance of immune response when these materials interact with the host tissues. It has therefore, become important to endow the implant materials with immunomodulatory properties favouring osteogenesis and osseointegration. Strontium, zinc and silicon are bioactive elements that have important roles in bone metabolism and that also elicit significant immune responses. In this study, Sr, Zn and Si-containing bioactive $Sr_2ZnSi_2O_7$ (SZS) ceramic coatings on Ti-6Al-4V were successfully prepared by a plasma-spray coating method. The SZS coatings exhibited slow release of the bioactive ions, with significantly higher bonding strength than hydroxyapatite (HA) coatings. SZS coated Ti-6Al-4V elicited significant effects on the immune cells, inhibiting the release of pro-inflammatory cytokines and fibrosis-enhancing factors, while upregulating the expression of osteogenic factors of macrophages. It could also inhibit the osteoclastic activities. The RANKL/RANK pathway, which enhances osteoclastogenesis, was inhibited by the SZS coatings, whereas the osteogenic differentiation of BMSCs was significantly enhanced by the SZS coatings/macrophages conditioned medium, probably via the activation of BMP2 pathway. SZS coatings are, therefore, a promising material for orthopaedic applications, and the strategy of manipulating the immune response by a combination of bioactive elements with controlled release has the potential to endow biomaterials with beneficial immunomodulatory properties.

Key words: SZS coatings; bonding strength; osteogenesis; inflammatory reaction; osteoclastogenesis, macrophages, bone marrow derived mesenchymal cells (BMSCs)

View Article Online
DOI: 10.1039/C4TB00837E

1. INTRODUCTION

The paradigm of the bone implant materials has shifted from being largely inert to having immunomodulatory properties and emphasizes the important role of immune responses during the biomaterial and host tissue interaction.[1] Inappropriate material-mediated immune response, such as excessive inflammation, may lead to the formation of fibrous capsule, which prevents the bone cells from contacting and integrating with the implants and result in the failure of implants.[2] As foreign bodies, implants will be recognised by the immune system, eliciting a foreign body reaction that may eventually form a fibrous capsule.

In addition to excessive inflammation, the immune response was also found to play an important role in the integration and functioning of the biomaterial. With the emergence of osteoimmunology, the immune and skeletal systems are found to be closely related, sharing a number of cytokines, receptors, signalling molecules and transcription factors. It is found that the combination of all four cytokines, tumor necrosis factor alpha (TNFα), transforming growth factor beta (TGFβ), interferon gamma (IFNγ), and interleukin 17 (IL-17), at physiological concentrations, can induce mineralized matrix as effectively as dexamethasone (a commonly used osteogenic medium supplement), and the loss of any of these cytokines leads to the loss of osteogenesis.[3] However, conditioned medium from lipopolysaccharide (LPS)-activated inflammatory M1 macrophages induced pre-osteoblast cells to differentiate towards fibroblasts even in the presence of osteogenic medium and this may be related to the upregulation of TNFα, IL-1β and IL-6.[4, 5] It has also been shown that upregulation of IFNγ and TNFα by T lymphocytes can lead to the failure of MSCs based bone tissue regeneration and that these effects can be attenuated by the application of the anti-inflammatory drug aspirin.[6] As for osteoclastogenesis, B cells are found to be the main source of bone marrow-derived osteoprotegerin (OPG, a decoy receptor for RANK receptor), with a percentage of 64%.[7, 8] T-cells are thought to work cooperatively with B-cells and enhance OPG production

View Article Online
DOI: 10.1039/C4TB00837E

via CD40/CD40L co-stimulation.[7] It is therefore of great interest and significance to endow materials with beneficial immunomodulatory properties for the development of advanced bone implant materials, so that the implanted biomaterial can facilitate an immune environment that is favourable for new bone regeneration and osseointegration.

Many types of immune cells participate in the induced immune response, such as mast cells, lymphocytes, dendritic cells and macrophages. Of these, macrophages are considered the most important effector cells, which play a major role in determining the long-term immune response to materials and therefore the outcome of the inflammatory reaction.[9, 10] In addition to their well-known effects on innate immune response, macrophages are also known to influence bone dynamics. As osteoclasts precursor cells, macrophages can differentiate into osteoclasts under osteoclastogenic condition, participating in the bone remodelling and material degradation. Macrophages also contribute to the osteogenesis, through the expression and secretion of a wide range of regulatory molecules, such as bone morphogenetic protein 2 (BMP2), TGFβ, and vascular endothelial growth factor (VEGF).[11, 12] Resident macrophages (osteomacs) are required for efficient osteoblast mineralization, and the depletion of macrophages leads to the complete loss of *in vivo* osteoblast-mediated bone formation.[13] Macrophages also release chemoattractants, such as chemokine (C-C motif) ligand 2 (CCL2) and CCL18, thereby participating in the recruitment of MSCs.[14] Therefore, the response of macrophages was applied as an indicator of immune response in this study.

Nutrient elements are of great physiological importance and the integration of nutrient elements in biomaterials, especially in bone implant materials, has been regarded as a sound strategy to endow biomaterials with improved bioactivity. For example, strontium (Sr) incorporated hydroxyapatite has been found to inhibit osteoclast activity and enhance ostegenesis, therefore expanding the application range of hydroxyapatite to patients with osteoporosis. Zinc (Zn) has been reported to have stimulatory effects on bone formation and

View Article Online
DOI: 10.1039/C4TB00837E

mineralization[15] and physiologically Zn deficiency can lead to the retardation of bone growth.[16, 17] Therefore, its incorporation into CaP biomaterials enhances their osteogenic capacity. Silicon (Si) is an essential trace element for metabolic processes associated with bone development,[18] and is known to locate at active calcification sites during the early mineralization process of bone growth.[19] Insufficient dietary Si in chicks will lead to deformities of the comb, skin, and bones, whereas dietary Si supplementation can inhibit the bone resorption in ovarectomized animals.[20] Aqueous Si has been shown to enhance the proliferation, differentiation and collagen production of osteoblasts[21] and the release of Si-containing ionic products from bioactive glass, bioceramics and coatings show similar stimulating effects in the proliferation and differentiation of bone-forming cells.

In addition to their effects on osteogenesis, Sr and Zn are also found to significantly affect the immune response. For example, Sr is found to suppress the expression of the pro-inflammation cytokines,[22, 23] whereas Zn-substituted ceramics can enhance the release of the anti-inflammatory cytokine IL-10, while reduce the expression of TNFα and IL-1β, which may be related the regulation of toll-like receptor 4 (TLR-4) pathway.[24-27] Patients with inflammatory diseases, such as rheumatoid arthritis, are associated with low plasma Zn concentrations and exhibit increased TNFα levels.[28] The supplementation of Zn can reverse such a pathological process.[29] It is, therefore, pertinent to modify otherwise inert bone implant materials with nutrient elements to endow them with beneficial immunomodulatory properties, thus avoiding excessive inflammation, and inducing a balance between osteoclastogenesis and osteogenesis that is better suited for the osseointegration and functioning of the implant materials.

Titanium is a commonly-used metal for the fabrication of bone implants and bioactive ceramic coatings are considered a feasible strategy to enhance its bioactivity. A number of bioactive ceramic coatings have been investigated, many of which have improved

View Article Online
DOI: 10.1039/C4TB00837E

bioactivity;[30, 31] however, most efforts have focused on the osteogenic properties, *vis-a-vis* the interaction with bone cells but not the immune response, in spite of the well-documented role of the latter during the osseointegration. In this study, we have sought to combine the potentially effective micronutrient elements (Sr, Zn and Si) into a bioceramic system, in an effort to impart beneficial immunomodulatory properties to the titanium metal substrate to modulate inflammation, osteoclastogenesis and enhance osteogenesis. We have recently prepared $Sr_2ZnSi_2O_7$ (SZS) ceramics.[32] In this study, the prepare SZS ceramics was further coated on the Ti-6Al-4V substratum via the plasma-spray method, for potential orthopaedic applications. The immunomodulatory property (including the inflammatory reaction, osteoclastogenesis and osteogenesis) and the possibly underlying mechanisms were systematically investigated.

2. EXPERIMENTAL SECTION

2.1 Preparation and characterization of SZS coatings on Ti-6Al-4V

The SZS powders were synthesized by the solid-state reaction process using SrO, ZnO and SiO_2 as raw materials according to our previous study.[32] To improve powder flowability, a sinter-crushing method was used. Briefly, the synthesized SZS powder was pressed into tablets, sintered at 1300^{o}C after which the sintered tablets were crushed and sieved by 200 and 400 meshes to obtain SZS particles with diameter of 40-80 μm for further coating preparation. The particle with the size of 40-80 μm has the most favorable powder flowability for the preparation of SZS coatings. The SZS powders and reconstituted particles were characterized by scanning electron microscopy (SEM, JSM-6700 F, Tokyo, Japan) and X-ray diffraction (XRD, D8 advance, Bruker, Germany).

To prepared SZS coatings, the reconstituted SZS particles were sprayed on Ti-6Al-4V disks with dimensions of 10×10×2 mm (Yantai Metallic Material Co., Ltd, Shanghai, China). Prior

View Article Online
DOI: 10.1039/C4TB00837E

to plasma spraying, the Ti-6Al-4V substrates were grit blasted, ultrasonically washed with ethanol and dried at 60°C. An atmosphere plasma spraying system (Sulzer Metco, Sulzer, Winterthur, Switzerland) was applied to fabricate SZS coatings, and the parameters for plasma sprayed SZS coatings were shown as following (argon plasma gas flow rate: 40 slpm, hydrogen plasma gas flow rate: 10 slpm, spray distance: 120 mm, argon powder carrier gas: 3.5 slpm, current: 700A, voltage: 66 V). The surface and cross-section of the prepared SZS coatings was observed by SEM. The crystal phase composition of the prepared SZS coatings was characterized by XRD. HA coatings were fabricated by spraying commercial HA powders onto Ti-6Al-4V substrate according to the previous study[33] and used as the control.

2.2 Bonding strength and solubility of SZS coatings

The bonding strength between SZS coatings and Ti-6Al-4V substrate was measured with a mechanical tester (Instron-5592, SATEC, New Jersey, USA) in accordance with American Society for Testing and Materials (ASTM) C-633 described previously.[34, 35] In brief, 10 cylindrical Ti-6Al-4V rods (diameter: 25.4 mm) were prepared. Half of the rods were spray coated with SZS (final coating mass: 0.0394 ± 0.0008 g), the other half were grit blasted. High-performance E-7 glue (Shanghai Institute of Synthetic Resin, Shanghai, China) was used to join the two rods (one with SZS coatings and the other grit blasted), and compressive stress applied to both ends to assure close contact, after which the rods were placed in an oven at 100 °C for 3 h to solidify the glue. The bonding strength was measured by a mechanical tester at a crosshead speed of 2 mm·min^{-1}, and the average of five measurements was calculated for the bonding strength of SZS coatings with the Ti-6Al-4V substrate.

To investigate the chemical stability of the SZS coatings, the samples were immersed in simulated body fluids (10 mL) and kept under shaking conditions at 37 °C for defined time periods. The ionic concentrations of Sr, Zn, Si, Mg, Ca and P ions in SZS-soaked buffer

View Article Online
DOI: 10.1039/C4TB00837E

solution were tested by inductively coupled plasma atomic emission spectroscopy (ICP-AES, Varian 715ES, California, USA).

2.3 Cell culture

Three cell types, the murine-derived macrophage cell line RAW 264.7 (RAW) cells, osteoclasts and BMSCs, were used in this study.[35] RAW cell cultures were maintained in Dulbecco's Modified Eagle Medium (DMEM, Life Technologies, Carlsbad, California, USA) supplemented with 5% fetal bovine serum (FBS, Thermo Scientific, Waltham, Massachusetts, USA), and 1% (v/v) penicillin/streptomycin (Life Technologies) (complete medium) at 37 ºC in a humidified CO_2 incubator. The cells were passaged at approximately 80% confluence by scraping and expanded through two passages before being used for the study.

Osteoclasts were derived from RAW cells following the protocol as previously described.[36] In brief, RAW cells were seeded to the T25 flask and cultured in complete medium for three days, after which the medium was replaced with fresh complete medium supplemented with 35 ng/ml of recombinant human receptor activator of nuclear factor kappa-B ligand (RANKL) (Millipore, Billerica, Massachusetts, USA). The medium was changed every 3 days and cells were allowed to differentiate into functional osteoclasts over a period of 21 days.

BMSCs were isolated and cultured based on protocols according to our previous studies.[37, 38] Briefly, bone marrow was obtained from patients (50-60 years old) undergoing hip or knee replacement surgery with informed consent given by all donors and the procedure was approved by the Ethics Committee of Queensland University of Technology. Lymphoprep was added to isolate the mononuclear cells from the bone marrow by density gradient centrifugation (Axis-Shield PoC AS, Oslo, Norway). The obtained cells were seeded into the tissue culture flasks containing DMEM supplemented with 10% FBS and 1% penicillin/streptomycin and incubated at 37 ºC in a humidified CO_2 incubator. The culture

View Article Online
DOI: 10.1039/C4TB00837E

medium was changed every 3 days until the primary mesenchymal cells reached 80% confluence. The unattached hematopoietic cells were removed through medium change. The confluent cells were routinely subcultured by trypsinisation. Only early passage cells (p3–5) were used in this study.

2.4 Ionic concentrations and the preparation of conditioned mediums

SZS and HA coated Ti-6Al-4V were immersed in the complete medium with or without cultured RAW cells. After 3 and 6 days, the conditioned mediums were collected, and centrifuged at 1500 rpm for 20 min at 4 ºC to clear the supernatants, which were then mixed with 0.5% HNO_3 at a ratio of 1:2 in preparation for the further ions concentration detection. The ionic concentrations of Sr, Si, Zn and Ca ions in complete culture medium, macrophages and osteoclasts conditioned mediums were quantified by ICP-AES . RAW cell conditioned mediums on day 3 were collected after clarified by centrifugation at 1500 rpm for 20 min. All the supernatants were then mixed with complete culture medium at a ratio of 1:2 to gain the RAW cells/coating materials conditioned mediums (CM), which were then kept in -80 ºC before further experiments.

2.5 The growth of RAW 264.7 cells on SZS-coated Ti-6Al-4V

RAW cells were seeded on the coating surface at a density of 10^5/coating disk (10×10mm). The cells were incubated for 1 day, then a MTT [3-(4,5-dimethylthiazol-2-yl)-2,5-diphenyl tetrazolium bromide] assay was applied to test the overall metabolic activity. 50 μL of 5 mg/mL MTT solution was added into each well then incubation for 4 hours. The DMEM-MTT solution was carefully removed. Images were captured to document the formation of formazan crystal and then 100 μL of dimethyl sulfoxide (DMSO) was added to each well to dissolve the formazan crystals for quantitative assay. Absorbance was read at 495 nm on a microplate spectrophotometer (Benchmark Plus, Tacoma, Washington, USA).

View Article Online
DOI: 10.1039/C4TB00837E

For fluorescence microscopy, the cells were washed with cold PBS twice before being fixed in 4% paraformaldehyde (PFA) for 15 mins at room temperature (RT) and then washed twice with PBS to remove the PFA. The cells were permeabilized with 0.1% Triton/PBS for 20 mins at RT. The cells were incubated in 1% BSA/PBS for 1 h and then 4',6-diamidino-2-phenylindole (DAPI) and phalloidin with fluorescein isothiocyanate (FITC) were added at 1:1000 and 1:250 dilution respectively to stain the nuclei and cytoskeletons and allowed to incubate in darkness for 20 min. Images were captured by confocal microscope (TCS SP5, Leica Microsystem, Solms, Germany).

2.6 The inflammatory response of RAW 264.7 cells cultured on SZS-coated Ti-6Al-4V

Inflammatory gene expression of RAW264.7 cells: RAW cells were seeded on coated surfaces at a density of 10^5/disk (10×10mm). After 7 hours of culture, total RNA was extracted using TRIzol reagent (Life Technologies) for RT-qPCR detection and 500 ng of total RNA used for the synthesis of complementary DNA using DyNAmo^{TM} cDNA Synthesis Kit (Finnzymes, Thermo Scientific) following the manufacturer's instructions. The cDNA was stored in -20 ºC for the further analysis of inflammatory and osteogenesis regulating gene expression.

RT-qPCR primers (Supporting information Table 1), which were designed based on cDNA sequences from the NCBI Sequence database. SYBR Green qPCR Master Mix (Life Technologies, Carlsbad, California, USA) was used for detection and the target mRNA expressions (*TNFα*, *IL-1β*, *IL-6*, *IFNγ*, *OSM*, *WNT5A*, *IL-10*, and *IL-1ra*) were assayed on the ABI Prism 7500 Thermal Cycler (Applied Biosystems, Foster City, California, USA). The cycle threshold (Ct) value of each target gene was normalized against Ct value of a house keeping gene (*GAPDH*) to gain the relative expression. For the calculation of fold change, ΔΔCt method was applied, comparing mRNA expressions between SZS coating group and HA coating group.

View Article Online
DOI: 10.1039/C4TB00837E

*Enzyme-linked immunosorbent assay (ELISA) of TNFα :*Supernatants were collected from RAW cells cultured on HA and SZS coated Ti-6Al-4V in previous section and the TNFα content was quantified using ELISA kits (R&D Systems, Minneapolis, Minnesota, USA) according to the manufacturer's instruction. All experiments were performed in triplicate. The TNFα concentration was determined by correlation with a standard curve and the results were expressed as the amount (pg) of TNFα per ml of supernatant.

2.7 Osteogenesis regulating gene expression of RAW 264.7 cells cultured on SZS-coated Ti-6Al-4V

The expressions of osteogenesis regulating genes macrophage colony-stimulating factor *(MSCF)*, *TGFβ1*, *TGFβ3*, *VEGF* and *BMP2* of RAW cells were detected by RT-qPCR, following the same method as previously described. cDNA used in this section was collected from previous section and *GAPDH* was applied as housekeeping gene.

2.8 The osteoclateogenesis and osteoclastic activities by the stimulation of SZS-coated Ti-6Al-4V

RAW cells were seeded on coated surfaces at a density of 10^5/disk (10×10mm). The cells were incubated for 1 day and then stained by DAPI and Phalloidin with FITC as previously described, to observe the phagocytosis of the coating materials. Osteoclasts were seeded on the coated surfaces at a density of 10^5/ disk. On day 3, total RNA was extracted using TRIzol reagent for detection of osteoclastic activities related gene expression tartrate-resistant acid phosphatase (*TRAP*), Cathepsin K (*CTSK*), Carbonic Anhydrase II (*CA 2*), receptor activator of NF-κB (*RANK*) and Calcitonin Receptor (*CT*), Matrix metalloproteinase-9 (*MMP9*)) as previously described. GAPDH was applied as housekeeping gene.

Given that osteoblast cells are an important source of osteoclastogenesis regulating cytokines, we further used the macrophage-conditioned mediums to stimulate the BMSCs to assay the

View Article Online
DOI: 10.1039/C4TB00837E

gene expression changes of osteoclastogenesis regulating cytokines. BMSCs were seeded in the 6 well plates and cultured in complete medium. After 1 day of culture, the medium was replaced by the CMs obtained from previous section. After 7 days, total RNA was extracted using TRIzol reagent. RT-qPCR detection was carried out to determine the osteoclastogenesis regulating cytokines (*MCSF*, *RANKL*, and *OPG*) gene expression changes as previously described. GAPDH was applied as housekeeping gene.

2.9 The osteogenic differentiation of BMSCs stimulated by RAW cells/coating materials conditioned mediums

Bone-related gene and protein expression of BMSCs: BMSCs were plated at a density of 20,000 cells per well in separate 6-well plates. After 24 hours of incubation, the culture medium was removed and replaced by CM. Cell morphology was observed under a Nikon's inverted microscope (Eclipse Ti, Nikon, Tokyo, Japan) and figures were taken. Total RNA was extracted using TRIzol reagent after 3 and 7 days of culture for detecting the expression of alkaline phosphatase *(ALP)*, osteopontin (*OPN)*, osteocalcin (*OCN)*, collagen 1 (*COL1)* genes using RT-qPCR as previously described. GAPDH was applied as housekeeping gene.

The whole cell lysates were collected after 14 days of culture, and analysed by Western blot. Fifteen micrograms of proteins from each sample were separated on SDS-PAGE gels and then transferred onto a nitrocellulose membrane (Pall Corporation, East Hills, New York, USA). The membranes were blocked in Odyssey blocking buffer for 1 hour (LI-COR Biosciences, Lincoln, Nebraska, USA), the membranes were incubated with primary antibodies against ALP (1:10,000, rabbit anti-human; Abcam, Cambridge, United Kingdom) and α-tubulin (1:5000, rabbit anti-human; Abcam) overnight at 4 °C. The membranes were washed three times in TBS-Tween buffer, and then incubated with anti- rabbit HRP conjugated secondary antibodies at 1: 4000 dilutions for 1 hour at room temperature. The protein bands were visualized using the Odyssey infrared imaging system (LI-COR Biosciences). The relative

View Article Online
DOI: 10.1039/C4TB00837E

intensity of protein bands was quantified using Image J software (National Institutes of Health, Bethesda, Maryland, USA).

The mineralization of BMSCs: Mineralization nodules were visualised by Alizarin Red S staining on day 14 after BMSCs grown in CM in well plates with osteogenic supplements. The medium was removed and the cells were washed with ddH_2O and fixed in 4% PFA for 10 min at room temperature. After gently rinsing with ddH_2O, the cells were stained in a solution of 2% Alizarin Red S at pH 4.1 for 20 min and were then washed with ddH_2O. The samples were air-dried and images taken under a light microscope.

Quantification of staining was done as previous described.[39] In brief, 350 μL 10% acetic acid was added to each well, and the plate was incubated at room temperature for 30 min. The monolayer was then scraped from the plate and transferred with the acetic acid to a 1.5 mL microcentrifuge tube. After vortexing for 30 s, the slurry was overlaid with 300 μL mineral oil (Sigma-Aldrich, St. Louis, Missouri, USA), heated to 85 °C for 10 min, and transferred to ice for 5 min. The slurry was then centrifuged at 20,000 g for 15 min and 300 μL of the supernatant was removed to a new 1.5 mL microcentrifuge tube. Then 100 μL of 10% ammonium hydroxide was added to neutralize the acid. Aliquots (100 μL) of the supernatant were read in triplicate at the wavelength of 405 nm in 96-well plates using a microplate spectrophotometer.

BMP2-related signalling pathway of BMSCs: BMSCs were plated at a density of 20,000 cells per well in separate 6-well plates. After 24 hours of incubation, the culture medium was removed and replaced by CM. Total RNA was extracted using TRIzol reagent after 3 days of culture. To investigate the activation of the BMP2 signalling pathway in BMSCs, BMP2 signalling pathway related genes [Mothers against decapentaplegic homolog 1/4/5 (*SMAD1*, *SMAD4*, *SMAD5*), bone morphogenetic protein receptor, type IA (*BMPR1A*) and bone

View Article Online
DOI: 10.1039/C4TB00837E

morphogenetic protein receptor type II (*BMPR2*)] were analysed by RT-qPCR as previously described.

2.10 Statistical analysis

All the analyses were performed using SPSS software (IBM SPSS, Armonk, New York, USA). Data is shown as means ± standard deviation (SD) and analysed using one-way ANOVA followed by LSD *post-hoc* test. The level of significance was set at $P<0.05$.

3. RESULTS

3.1 Characterization, bonding strength and solubility of SZS particles and coatings

The particle size of synthesized SZS powders was no more than 5 μm with irregular shapes (Fig. 1A). After reconstituted by sinter-crushing method, the SZS particles became larger in size (around 40-80 μm), with relatively regular shape (Fig. 1B). Although there were a few impurities of Sr_2SiO_4 phase in the SZS powders, the particles were pure with respect to the $Sr_2ZnSi_2O_7$ crystal phase (Fig. 1C). The surface and cross-section morphology of the SZS coatings are shown in Figure 1D and 1E. The coatings had a dense surface that consisted of stacks of fully melted SZS particles (Fig. 1D). The thickness of the coatings was around 100μm (Fig. 1E). XRD analysis showed that the main crystal phase of the SZS coatings was $Sr_2ZnSi_2O_7$ with small amount of Sr_2SiO_4 (Fig. 1F). The mean bonding strength of the SZS coatings with Ti-6Al-4V substrate was 34.3±1.9 MPa.

After soaking in a phosphate-buffered solution for 14 days, the SZS coatings showed no significant degradation (Fig. 2A). Sr and Si concentrations in the phosphate-buffered solution increased significantly after the first 2 days of soaking and then decreased over the duration of soaking time. Zn, Ca, P and Mg concentrations showed no significant changes during the whole soaking period (Fig. 2B).

View Article Online
DOI: 10.1039/C4TB00837E

3.2 The growth of RAW 264.7 cells on SZS-coated Ti-6Al-4V

More formazan crystals were formed on the HA coated surfaces than the SZS surfaces, which was confirmed by the quantitative detection, showing that HA group had higher mean OD value (Fig. 3 A). Fluorescent microscopy revealed a similar trend that more RAW cells were observed on the HA coating surfaces than the SZS surfaces (Fig. 3 B, C).

3.3 The inflammatory response of RAW 264.7 cells cultured on SZS-coated Ti-6Al-4V

The pro-inflammatory genes *TNFα*, *IFNγ*, Oncostatin M (*OSM*) expression was significantly downregulated in RAW cells subjected to stimulation by the SZS coating compared with the HA coating group (Fig. 4 A, D, E, $P<0.05$). TNFα ELISA result showed similar trend, with the decrease of TNFα released in the mediums (Fig. 4 I). However, *IL- 6* gene expression was slightly increased, while *IL-1β* showed no significant change with same treatment (Fig. 4 B, C). The gene expression of the pro-inflammatory indicator *WNT5A* showed significant downregulation (Fig. 4 F, $P<0.05$), whereas the anti-inflammatory gene *IL-10* was significantly upregulated by the stimulation of SZS coatings in comparison with the HA coating groups ($P<0.05$) (Fig. 4 G). *IL-1ra*, by contrast, was significantly downregulated with the same treatment ($P<0.05$) (Fig. 4 H).

3.4 Osteogenesis regulating gene expression of RAW 264.7 cells cultured on SZS-coated Ti-6Al-4V

Both osteoclastogenesis-enhancing (MCSF) and fibrosis-enhancing (TGFβ1 and TGFβ3) factors were all significantly downregulated (Fig. 5 A, B, C, $P<0.05$). By comparison, the osteogenesis-enhancing factors VEGF and BMP2 were both significantly upregulated (Fig. 5 D, E, $P<0.05$).

3.5 The osteoclastic activities and osteoclastogenesis by the stimulation of SZS-coated Ti-6Al-4V

View Article Online
DOI: 10.1039/C4TB00837E

RAW cells showed higher phagocytotic activity on the HA coated surfaces than on the SZS coated surfaces. The cells appeared to internalize the HA particles, forming a big "bubble" within the cytoplasma, which can be seen in most of the stimulated cells (Fig. 6 A, B). By contrast, this observation was not generally seen in the SZS coating stimulating RAW cells (Fig. 6 C, D).

All osteoclast related genes (*TRAP*, *CTSK*, *CAR2*, *RANK*, and *MMP9*) by osteoclasts were significantly downregulated as a result of stimulation by the SZS coating compared with that of HA coating (Fig. 7 A). The expression of osteoclastogenesis enhancing gene *RANKL* by BMSCs was significantly downregulated (Fig. 7 B, $P<0.05$), while another osteoclastogenesis enhancing gene MCSF was slightly upregulated (Fig. 7 B, $P<0.05$). The expression of the osteoclastogenesis inhibiting gene *OPG* was significantly upregulated (Fig. 7 B, $P<0.05$).

3.6 The osteogenic differentiation of BMSCs stimulated by RAW 264.7 cells/coating materials-conditioned mediums

BMSCs grew well in both HA and SZS CM (Supporting information Fig. 1). Expression of two measured mineralization-related genes (*OPN*, *COL1*) by BMSCs stimulated by SZS CM were significantly upregulated compared to HA CM on both day 3 and day 7 (Fig. 8, $P<0.05$). Similarly, *ALP* gene expression was upregulated on day 3, and *OCN* gene expression was upregulated on day 7 (Fig. 8, $P<0.05$). However, *ALP* and *OCN* gene expressions showed no significant changes on day 3 and 7, respectively (Fig. 8, $P>0.05$). Western blot of ALP showed that ALP protein expression was significantly upregulated by BMSCs stimulated by SZS CM compared to HA CM (Fig. 9 A, $P<0.05$).

Alizarin Red S staining showed evidence of calcium deposition and nodule formation. Mineralized nodules were observed in both groups with osteogenic medium (Fig. 9). More distinct nodules were observed in BMSCs stimulated by SZS CM compared to that of HA

View Article Online
DOI: 10.1039/C4TB00837E

CM, which was confirmed by the quantitative detection, which showed that the SZS group had higher absorbance value than the HA group (Fig. 9 B, $P<0.05$).

3.7 BMP2 signalling pathway-related gene expression

To further explore the mechanism of the enhanced osteogenesis, we examined the gene expressions of BMP2 signalling pathways. The expressions of *BMPR2*, *SMAD1*, *SMAD4* and *SMAD5* in BMSCs cultured in SZS CM showed significantly upregulation compared to those cultured in HA CM (Fig. 10, $P<0.05$). However, the expression of *BMP1A* in BMSCs cultured in SZS CM was significantly downregulated compared to those cultured in HA CM (Fig. 10, $P<0.05$).

3.8 Ionic concentrations of conditioned mediums

Sr, Si and Zn ionic concentrations in the culture mediums were all significantly higher after soaking the SZS coated Ti-6Al-4V at both day 3 and 6 compared with that of HA coated Ti-6Al-4V, independent of whether or not cells had been cultured on the disks (macrophages and osteoclasts) (Table 1). Sr concentrations showed the most significant increase, up to approximately 450 ppm. Si and Zn concentration were much lower, at around 60 and 45 ppm. Ca concentrations for the SZS groups were all lower than the HA groups (Table 1).

4. DISCUSSION

Bone biomaterials, such as titanium, can safely remain inside the body throughout life without triggering any significant immune response. However, such implants act simply as an “inert” mechanical support and can, therefore, not meet the specifications of an ideal bone biomaterial. For this reason it is of great importance to endow bone biomaterials with beneficial immunomodulatory properties, so that they can create a favourable immune environment to induce desired osseointegration and osteogensis. In this study, we have

View Article Online
DOI: 10.1039/C4TB00837E

attempted to endow Ti-6Al-4V with a immunomodulatory function by coating with nutrient elements-based $Sr_2ZnSi_2O_7$ bioceramics. The induced immunomodulatory activities showed significant effects on the downregulation of inflammation, inhibition of osteoclastogenesis, and enhancement of osteogenesis (Figure 11).

4.1 Nutrient elements released from the $Sr_2ZnSi_2O_7$ coating

According to the data sheet from the manufacturer, DMEM contains very few amounts of Sr, Zn and Si ions, and the major ions contained are Ca^{2+}, Mg^{2+}, K^+, Na^+, Cl^-, PO_4^{3-} *etc*. When SZS coating is in contact with culture medium, Sr, Zn, and Si ions are largely unsaturated in the solvent (culture medium), which leads to a relatively rapid releasing of Sr, Zn, and Si ions into the culture medium at the early stage of soaking.

The molar ratio of Sr/Zn/Si in the immersed culture medium is around 7:1:3, different from the stoichiometric ratio (2:1:2), which may be due to the incongruent dissolution of Sr, Zn, and Si ions. SZS coating has a polycrystal structure and the dissolution is influenced by its crystal morphology and surface microstructure. Thus, the release of Sr, Zn and Si ions does not follow the stoichiometric ratio of material composition. In addition, due to the existence of surface microstructure deformities and unstable glass phase of SZS coatings, the dissolution rate of SZS coatings in DMEM is faster during the early stage, which may account for the higher Sr ion concentration at day 3 compared with that of day 6. It seems that Sr and Si dissolution are faster than for Zn, leading to the higher proportion of Sr and Si in the immersed culture medium.

As to the long-term dissolution of SZS coating, the accumulative releasing rates of SZS coating over 14 days in SBF are Si: ~2.94%, Sr: ~5.78%, Zn ~0.90% (caltulated from Figure 2 B). The releasing of Sr, Zn and Si shows different rate at the beginning (0-2 days Si: ~1.81%, Sr: ~2.88%, Zn ~0.14%; 2-4 days Si: ~0.22%, Sr: ~1.16%, Zn ~0.14%). Sr has the

View Article Online
DOI: 10.1039/C4TB00837E

highest releasing rate while Zn has the lowest releasing rate. As time goes on (6-14 days), all three ions show slow releasing manner in a steady rate (Si: ~0.15%, Sr: ~0.3%, Zn ~0.12%), something which is important to eliciting a sustained effect on the surrounding cells and maintains the long-term useful life of implants. When the bioceramic coated implants are implanted *in vivo*, host body cells will be in contact with the coating materials first. The coating materials will then experience some degradation either by physicochemical dissolution, cell-medicated dissolution, hydrolysis, enzymatic decomposition, or corrosion.[40] The released ions or degraded particles from the coating are supposed to regulate the local microenvironment and determines the response and behaviour of host cells. It is therefore, vital to coat the titanium surface with bioactive materials that can create an environment favourable for the new bone formation, like SZS did in this study. To maintain the long-term life span of the implants, bioceramic coatings should have a slow release of bioactive ions at sufficient concentrations to assist osseointegration with the host bone tissue. Fast degradation would not provide sufficient time for the osseointegration, and might also result in adverse effects due to the high concentrations of releasing ions. In the present study, SZS had a greater ability to inhibit osteoclastogenesis than did HA, suggesting that SZS coatings may impose greater biological stability than does HA coatings.

4.2 How do the released nutrient elements modulate the immune response?

Zn is well known to be essential for the normal development and function of immune cells.[41] Zn deficiency will lead to the impairment of the production and signalling of inflammatory cytokines and thereby affect the immunological functions.[42, 43] Plasma Zn concentration is maintained within a physiological range of 10-18 μmol/L (0.65-1.17 ppm) in homeostatic status.[43] During an inflammatory response, the Zn homeostasis is restored with the Zn redistributed into the cellular compartment, resulting in the rapid clearing of plasma Zn concentration and an increase of inflammatory cytokines (TNFα, IL-1β, IL-6).[44, 45] Low

View Article Online
DOI: 10.1039/C4TB00837E

plasma Zn concentration has become one common diagnostic feature of some inflammatory diseases (*e.g.* pneumonia and tuberculosis) and Zn supplementation (>45mg Zn/day) has been successfully applied as a therapeutic and preventive agent for these conditions, by decreasing the generation of pro-inflammatory cytokines.[41, 43] SZS coating, which is effectively a large storage of Zn, has a slow release of Zn ions during the interaction between macrophages and the implants, and results in dampening the otherwise excessive inflammatory response to exogenous bodies.

Zn affects the immune cells' response in a concentration-dependent manner. It was found that the addition of Zn resulted in a concentration-dependent stimulation of TNFα (peaking at 250 μmol/L (16.25 ppm)) and IL-1β (peaking at 120 μmol/L (7.8 ppm)) in peripheral blood mononuclear cells.[46] In addition, 100 μmol/L (6.5 ppm) is supposed to be minimum concentration to inhibit the growth of peripheral blood mononuclear cells.[47] Therefore, high concentration of Zn in the conditioned medium (45 ppm (690 μmol/L)) may be a key reason for the inhibition of macrophage growth and the dampening of the inflammatory response.

Sr is known to stimulate osteogenesis and suppress osteoclastogenesis, with the underlying mechanism supposed to be related to antagonizing the activation of nuclear factor kappa-light-chain-enhancer of activated B cells (NF-κB).[48] NF-κB is known to play a key role in activating the inflammatory response, which suggests that Sr probably has some anti-inflammatory effects. Some studies have been carried out to investigate whether introducing Sr into calcium phosphate based materials can modulate the immune response.[22, 49] It has been found that Sr doped calcium phosphate can inhibit the release of pro-inflammatory cytokine TNFα compared with HA, at both high (around 500 μmol/L) and low (10 μmol/L) Sr ion concentrations.[22, 49] IL-6, on the other hand, shows different expression patterns depending on Sr ion concentrations: at high concentration (around 500 μmol/L) Sr has a stimulatory effect on the release of IL-6,[49] whereas the opposite effect was observed at a low Sr ion

View Article Online
DOI: 10.1039/C4TB00837E

concentration (10 μmol/L).[22] Our results showed that TNFα was inhibited and IL-6 was enhanced by SZS coating, which could be attributed to a high Sr concentration at approximately 450 ppm or 5.1 mmol/L.

Ca is another element that is known to have modulatory effects on the immune response. One of the underlying mechanism is supposed to be related to the WNT5A/Ca^{2+} pathway, which is known to enhance the inflammation when activated.[50] Wnt5A can bind to Fz5, activating the Wnt/Ca^{2+} signalling pathway via calmodulin-dependent protein kinase II (CaMKII) and protein kinase C, which activates the expression of downstream inflammatory cytokine genes via the NF-κB transcription factor.[50] The culture medium showed a significant decrease of Ca^{2+} concentration after SZS coated implants had soaking in it. It is a reasonable to speculate that the decreased concentration of Ca^{2+} could be responsible for inhibiting the Wnt/Ca^{2+} signalling pathway, resulting in the anti-inflammatory effects.

Although the individual effect of each ion is well investigated, the synergistic effects of these ions are still largely unknown. Given both Zn and Sr have anti-inflammatory effects, it is reasonable to speculate that they can synergistically inhibit the inflammation under proper ionic concentrations. Our study demonstrated that the overall inhibitory effects of Zn (45 ppm (690 μmol/L)), Sr (450 ppm (5.1 mmol/L)), Si (58.86 ppm (2.1 mmol/L)) and Ca (43.05 ppm (1.08 mmol/L)) on inflammation. It seems the mixture of these ions (the ratio of Sr/Zn/Si is around 7:1:3) did not at least attenuate the original anti-inflammatory effects of Zn Sr and Ca. However, systemic study is required to find out whether the mixture of these ions at adequate concentration can synergistically modulate a favourable immune environment to enhance osteogenesis.

As was pointed out in the introduction, inflammatory response is a key factor in determining the formation of fibrous capsule.[9, 10] Excessive inflammation leads to the formation of fibrous capsule and can prevent the bone cells from contacting and integrating with the implants, thus

View Article Online
DOI: 10.1039/C4TB00837E

resulting in implant failure.[2] The inhibition of an inflammatory response indicates that the SZS coatings are more compatible than HA coatings and may prevent the formation of fibrous capsule.

4.3 The effects of the modulated immune environment on osteoclastogenesis

The immune environment created by SZS coated Ti-6Al-4V appears to inhibit the osteoclastic activities and osteoclastogenesis. TRAP, CTSK, CA2, RANK, and MMP9 are recognised as markers of osteoclast activity. TRAP is highly expressed by osteoclasts and activated macrophages and its expression is increased when osteoclastic activity is enhanced. CTSK is a gene encodes a lysosomal cysteine protease involved in bone remodelling and resorption, which is expressed predominantly in osteoclasts. CA2 plays an important role in osteoclast differentiation and bone resorption by effecting the steady state intracellular pH and Ca^{2+}. MMP9 is a protease involving in the breakdown of bone matrix. Therefore, the downregulation of these genes can well indicate that the osteoclatic activities were suppressed.

The osteoclastogenesis is also known to be regulated by the RANKL/RANK/OPG pathway. RANKL binds to RANK, a receptor on the surface of osteoclast precursors, activating signalling through NF-κB, activator protein 1 (AP-1) and nuclear factor of activated T cells 2 (NFAT2) to induce expression of genes for the survival and differentiation of osteoclasts.[51] OPG, a decoy receptor derived from osteoblasts, can bind to RANKL and interrupt its interaction with RANK receptor, thereby inhibiting osteoclastogenesis.[52, 53] In addition, MCSF is another factor involved in the maturation of osteoclasts. MCSF binds to its receptor, c-fms, on osteoclast precursors and activates signalling through the protein kinase B and mitogen-activated protein kinases pathway.[54] Osteoblastic cells are thought to be the major source of RANKL, MCSF and OPG, thus playing key role in regulating osteoclastogenesis. When compared to the HA coatings, it was found that SZS coatings could downregulate the

View Article Online
DOI: 10.1039/C4TB00837E

expression of RANKL gene, while upregulating the OPG expression of BMSCs, indicative of SZS coatings inhibiting osteoclastogenesis.

The inhibitory effects of Sr in the RANKL/RANK system have been well documented. Sr is found to inhibit the differentiation of osteoclast in a concentration dependent manner (0-200 μmol/L,[48] 0-24 mmol/L[55]), with higher concentration showing the most pronounced effect and thought to be related to the suppression of NFκB. The suppression of NFκB results in the downregulation of TNFα expression, and is implicated in the recruitment and differentiation of osteoclast precursors.[48] Although IL-6 has been linked to osteoclast differentiation and activity, the present study did not reveal any association between the upregualtion of IL-6 and osteoclast activity. In fact, IL-6 has been observed to have an inhibitory effect on osteoclast differentiation, indicating a multifunctional role of this cytokine.[56] In this study, the concentrations of the released Sr^{2+} in the macrophage-conditioned medium went as high as 483 ppm (5.52 mmol/L) for SZS coatings, which is significantly higher than that of the HA coatings (only 0.75 ppm) (as shown in Table 1), and resulted in the downregulation of TNFα expression and upregulation of IL-6. Therefore, it is reasonable to hypothesize that the possible mechanism for the downregulated osteoclastogenesis of SZS coatings is predominantly due to the released Sr^{2+} ions from the coatings and a subsequent alteration of the immune environment.

The successful osseointegration requires adequate and effective osteoclastic activities. High osteoclast activity may result in poor quality *de novo* bone tissue in terms of mass and density, which impedes the loading capacity of implants. Such a phenomenon is not uncommon clinically, especially in patients with osteoporosis. The inhibition of osteoclastogenesis may help to obtain properly balanced osteoclastogenesis and osteogenesis, extending the applications of SZS coated Ti-6Al-4V to patients with low bone mass and density, especially those with osteoporosis.

View Article Online
DOI: 10.1039/C4TB00837E

4.4 The effects of the modulated immune environment on osteogenesis

In addition to its effects on osteoclastic activities and osteoclastogenesis, the immune environment created by SZS coated Ti-6Al-4V also appears to elicit positive effects on the osteogenesis. ALP, OPN and COL1 are early markers of the osteoblast lineage while OCN is thought to be pinpointing of a more mature osteoblastic phenotype.[57] Therefore, it is reasonable to observe that ALP, OPN and COL1 were upregulated in the early stage (day-3), while OCN was upregulated only in the late stage (day-7). The osteogenic effects may be related to the upregulation of BMP2 and VEGF. BMP2 is a member of the transforming growth factor family and has a strong osteoinductive effect.[58, 59] On receptor activation, BMP2 transmit signals through SMAD-dependent and SMAD-independent pathways, leading to osteoblast differentiation of MSCs.[60] Macrophages are an important source of BMP2, contributing to osteogenesis during bone healing.[5] In this study, we found that SZS coatings significantly upregulated the BMP2 expression by macrophages. BMP2 binds to BMPR2 on the cell surface, which leads to the intracellular activation of SMAD5.[60] Activated SMAD5 subsequently form a complex with SMAD4, which translocates into the nucleus, where it facilitates the expression of distalless homeobox5 (Dlx5).[60] Dlx5 has been shown to induce the expression of Runt-related transcription factor 2 (Runx2), inducing osteogenic differentiation of BMSCs.[60] In addition, VEGF gene expression was also significantly upregulated, and its expression has been found to be tightly related and synergistic with that of BMP2.[61] VEGF reportedly enhances BMP2-induced osteogenesis and the inhibition of VEGF could block BMP2-induced angiogenesis and BMP4-induced bone formation.[62] Bone matrix deposition within the implants is another key step for the osseointegration. Materials enhancing osteogenesis would be of great significance in improving the quality of *de novo* bone by increasing its mass and density.

View Article Online
DOI: 10.1039/C4TB00837E

As profibrotic cytokines, TGF-βs were found to be highly expressed in a wide range of fibrous tissues. TGF-βs can promote the fibrosis process via upregulating the synthesis of many extracellular matrix (ECM) proteins.[63] TGF-β1, which induces fibroblast proliferation via the fibroblast growth factor 2/extracellular signal-regulated kinases (ERK) pathway, is a key cytokine in the fibrosis process.[64] TGF-β3 plays an important role in ECM production by inducing the expression of collagen type 1, fibronectin, laminin, and proteoglycans.[65] In addition, TNFα contributes to fibrosis via the mediator TNFR2, which then acts through ERK1/2 to stimulate proliferation of fibroblasts and inhibit collagen degradation.[66] TNFα was also found to activate the ERK-specific mitogen-activated protein kinase pathway, leading to the increased production of TGF-β1 in fibroblasts.[67] We assayed the expression of the fibrosis-promoting genes *TGF-β1*, *TGF-β3* and *TNFα*, which were all significantly downregulated, indicating that the SZS coated Ti-6Al-4V created immune environment did not enhance inflammatory fibrosis, but was effective and adequate in improving osteogenesis.

4.5 Bonding strength of the SZS coating

In addition to its favourable immunomodulatory property, the SZS coating also had a superior bonding strength. The bonding strength of bioceramic coatings with titanium is another important factor to maintain the effective life spans of the implants, since the high bonding strength will provide a stable coating interface without delamination from titanium to support functional loading before the coating materials are completely replaced by new bone tissue. The bonding strength of HA coatings is generally in the range of 15-25 Mpa. Although the HA coated implants have achieved certain clinical success, the bonding strength of HA coating on titanic alloy is still not strong enough and may lead to the delamination phenomenon in clinical applications. The clinical significance of higher bonding strengths cannot be underestimated and the SZS was shown to have a value of 34.3 MPa. This greater

View Article Online
DOI: 10.1039/C4TB00837E

bonding strength gives SZS coatings additional potential for clinical applications, since they may have longer life span with functional loading.

Therefore, Ti-6Al-4V coated with $Sr_2ZnSi_2O_7$ appears to have qualities that make it a promising material for orthopedic applications. In addition, the strategy applied in this study, which successfully endowed Ti-6Al-4V with immunomodulatory properties by the action of the Sr, Zn, Si bioactive elements in $Sr_2ZnSi_2O_7$, suggests a method of endowing otherwise inert biomaterials with immunomodulatory properties that results in a less severe immune response (Figure 11). However, further studies are needed to investigate the exact effects of bioactive elements with respect to immune response and osteogenesis by means of a systemic evaluation. This would provide basic knowledge for wider application of this strategy to manipulate the immune response by the use of different combinations of bioactive elements with controlled release.

5. CONCLUSIONS

In this study, SZS coatings on Ti-6Al-4V containing the bioactive elements Sr, Zn and Si have been successfully prepared by plasma-spray method. SZS coating endowed Ti-6Al-4V with immunomodulatory properties had the desirable effect of inhibiting the inflammatory reaction of RAW 264.7 immune cells. The SZS-induced immune microenvironments suppressed osteoclastogenesis and osteoclastic activities but enhanced the osteogenic differentiation via BMP2 pathway. In addition, the prepared SZS coatings had good chemical stability in phosphate-buffered solutions, and had significantly higher bonding strength than that of HA coatings. The excellent immunomodulatory and physicochemical properties of SZS coatings suggest that it is is a promising implant material for the orthopaedic applications. The strategy of manipulating the immune response by the use of defined combinations of bioactive elements, coupled with the controlled release of ions, can be

View Article Online
DOI: 10.1039/C4TB00837E

applied to endow these materials with beneficial immunomodulatory properties and improved osseointegration.

Acknowledgements

Funding for this study was provided by the Queensland-Chinese Academy of Sciences Collaborative Science Fund 2014, the Recruitment Program of Global Young Talent, China (C.W.), Shanghai Pujiang Talent Program (12PJ1409500), Natural Science Foundation of China (Grant 31370963, 81201202 and 81190132), Innovative Project of SIC, CAS, Australian Dental Research Foundation, and ARC (DP120103697). The authors wish to thank Dr. Thor Friis for his contribution in the preparation of the manuscript.

View Article Online
DOI: 10.1039/C4TB00837E

REFERENCES

1. S. Franz, S. Rammelt, D. Scharnweber and J. C. Simon, *Biomaterials*, 2011, 32, 6692-6709.
2. U. Walschus, A. Hoene, H. G. Neumann, L. Wilhelm, S. Lucke, F. Luthen, J. Rychly and M. Schlosser, *Acta Biomater*, 2009, 5, 776-784.
3. L. Rifas, *J Cell Biochem*, 2006, 98, 706-714.
4. F. Zheng, Ohio State University, 2010.
5. C. M. Champagne, J. Takebe, S. Offenbacher and L. F. Cooper, *Bone*, 2002, 30, 26-31.
6. Y. Liu, L. Wang, T. Kikuiri, K. Akiyama, C. Chen, X. Xu, R. Yang, W. Chen, S. Wang and S. Shi, *Nat Med*, 2011, 17, 1594-1601.
7. Y. Li, G. Toraldo, A. Li, X. Yang, H. Zhang, W. P. Qian and M. N. Weitzmann, *Blood*, 2007, 109, 3839-3848.
8. R. Pacifici, *Arch Biochem Biophys*, 2010, 503, 41-53.
9. M. Bartneck, K. H. Heffels, Y. Pan, M. Bovi, G. Zwadlo-Klarwasser and J. Groll, *Biomaterials*, 2012, 33, 4136-4146.
10. F. Variola, J. H. Yi, L. Richert, J. D. Wuest, F. Rosei and A. Nanci, *Biomaterials*, 2008, 29, 1285-1298.
11. Y. Honda, T. Anada, S. Kamakura, M. Nakamura, S. Sugawara and O. Suzuki, *Biochem Biophys Res Commun*, 2006, 345, 1155-1160.
12. S. M. Wahl, N. McCartney-Francis, J. B. Allen, E. B. Dougherty and S. F. Dougherty, *Ann N Y Acad Sci*, 1990, 593, 188-196.
13. M. K. Chang, L. J. Raggatt, K. A. Alexander, J. S. Kuliwaba, N. L. Fazzalari, K. Schroder, E. R. Maylin, V. M. Ripoll, D. A. Hume and A. R. Pettit, *J Immunol*, 2008, 181, 1232-1244.
14. O. M. Omar, C. Graneli, K. Ekstrom, C. Karlsson, A. Johansson, J. Lausmaa, C. L. Wexell and P. Thomsen, *Biomaterials*, 2011, 32, 8190-8204.
15. M. Yamaguchi, *J Trace Elem Exp Med*, 1998, 11, 119-135.
16. H. S. Hsieh and J. M. Navia, *J Nutr*, 1980, 110, 1581-1588.
17. J. T. Kim, S. H. Baek, S. H. Lee, E. K. Park, E. C. Kim, I. S. Kwun and H. I. Shin, *J Med Food*, 2009, 12, 118-123.
18. E. M. Carlisle, *Nutr Rev*, 1982, 40, 193-198.
19. E. M. Carlisle, *Science*, 1970, 167, 279-280.
20. F. H. Nielsen and R. Poellot, *J Trace Elem Exp Med*, 2004, 17, 137-149.
21. A. M. Pietak, J. W. Reid, M. J. Stott and M. Sayer, *Biomaterials*, 2007, 28, 4023-4032.
22. E. Buache, F. Velard, E. Bauden, C. Guillaume, E. Jallot, J. M. Nedelec, D. Laurent-Maquin and P. Laquerriere, *Acta Biomater*, 2012, 8, 3113-3119.
23. P. Romer, B. Desaga, P. Proff, A. Faltermeier and C. Reicheneder, *Ann Anat*, 2012, 194, 208-211.
24. A. Grandjean-Laquerriere, P. Laquerriere, E. Jallot, J. M. Nedelec, M. Guenounou, D. Laurent-Maquin and T. M. Phillips, *Biomaterials*, 2006, 27, 3195-3200.
25. R. M. Day and A. R. Boccaccini, *J Biomed Mater Res A*, 2005, 73, 73-79.
26. H. Haase and L. Rink, *Biometals*, 2007, 20, 579-585.
27. F. Velard, J. Braux, J. Amedee and P. Laquerriere, *Acta Biomater*, 2013, 9, 4956-4963.
28. P. Connell, V. M. Young, M. Toborek, D. A. Cohen, S. Barve, C. J. McClain and B. Hennig, *J Am Coll Nutr*, 1997, 16, 411-417.
29. A. Zoli, L. Altomonte, R. Caricchio, A. Galossi, L. Mirone, M. P. Ruffini and M. Magaro, *Clin Rheumatol*, 1998, 17, 378-382.
30. B. A. van Oirschot, H. S. Alghamdi, T. O. Narhi, S. Anil, A. Al Farraj Aldosari, J. J. van den Beucken and J. A. Jansen, *Clin Oral Implants Res*, 2014, 25, 21-28.

View Article Online
DOI: 10.1039/C4TB00837E

31. V. Cannillo, F. Pierli, S. Sampath and C. Siligardi, *J Eur Ceram Soc*, 2009, 29, 611-619.
32. M. Zhang, C. Wu, K. Lin, W. Fan, L. Chen, Y. Xiao and J. Chang, *J Biomed Mater Res A*, 2012, 100, 2979-2990.
33. C. Wu, Y. Ramaswamy, X. Liu, G. Wang and H. Zreiqat, *J R Soc Interface*, 2009, 6, 159-168.
34. D. Yi, C. Wu, X. Ma, H. Ji, X. Zheng and J. Chang, *Biomed Mater*, 2012, 7, 065004.
35. C. Wu, Z. Chen, D. Yi, J. Chang and Y. Xiao, *ACS Appl Mater Interaces*, 2014, 6, 4264-4276.
36. P. Collin-Osdoby and P. Osdoby, *Methods Mol Biol*, 2012, 816, 187-202.
37. Z. Chen, C. Wu, W. Gu, T. Klein, R. Crawford and Y. Xiao, *Biomaterials*, 2014, 35, 1507-1518.
38. Z. Chen, C. Wu, J. Yuen, T. Klein, R. Crawford and Y. Xiao, *J Biomed Mater Res A*, 2014, 102, 2813-2823.
39. C. A. Gregory, W. G. Gunn, A. Peister and D. J. Prockop, *Anal Biochem*, 2004, 329, 77-84.
40. M. Bohner, L. Galea and N. Doebelin, *J Eur Ceram Soc*, 2012, 32, 2663-2671.
41. A. S. Prasad, *Curr Opin Clin Nutr Metab Care*, 2009, 12, 646-652.
42. A. S. Prasad, *Mol Med*, 2008, 14, 353-357.
43. M. Foster and S. Samman, *Nutrients*, 2012, 4, 676-694.
44. N. E. Krebs and K. M. Hambidge, *Biometals*, 2001, 14, 397-412.
45. C. Lang, C. Murgia, M. Leong, L. W. Tan, G. Perozzi, D. Knight, R. Ruffin and P. Zalewski, *Am J Physiol Lung Cell Mol Physiol*, 2007, 292, L577-584.
46. P. Scuderi, *Cell Immunol*, 1990, 126, 391-405.
47. K.-L. Chang, T.-C. Hung, B.-S. Hsieh, Y.-H. Chen, T.-F. Chen and H.-L. Cheng, *Nutrition*, 2006, 22, 465-474.
48. M. Yamaguchi and M. N. Weitzmann, *Mol Cell Biochem*, 2012, 359, 399-407.
49. C. Cardemil, I. Elgali, W. Xia, L. Emanuelsson, B. Norlindh, O. Omar and P. Thomsen, *PLoS One*, 2013, 8, e84932.
50. A. De, *Acta Biochim Biophys Sin*, 2011, 43, 745-756.
51. M. Zaidi, *Nat Med*, 2007, 13, 791-801.
52. H. L. Wright, H. S. McCarthy, J. Middleton and M. J. Marshall, *Curr Rev Musculoskelet Med*, 2009, 2, 56-64.
53. B. F. Boyce and L. Xing, *Arthritis Res Ther*, 2007, 9 Suppl 1, S1.
54. M. Nakamura, A. Nagai, T. Hentunen, J. Salonen, Y. Sekijima, T. Okura, K. Hashimoto, Y. Toda, H. Monma and K. Yamashita, *ACS Appl Mater Interfaces*, 2009, 1, 2181-2189.
55. A. Caudrillier, A. S. Hurtel-Lemaire, A. Wattel, F. Cournarie, C. Godin, L. Petit, J. P. Petit, E. Terwilliger, S. Kamel, E. M. Brown, R. Mentaverri and M. Brazier, *Mol. Pharmacol.*, 2010, 78, 569-576.
56. F. Yoshitake, S. Itoh, H. Narita, K. Ishihara and S. Ebisu, *J Biol Chem*, 2008, 283, 11535-11540.
57. K. Kaveh, R. Ibrahim, Z. A. Bakar and T. A. Ibrahim, *J Anim Vet Adv*, 2011, 10, 2317-2330.
58. O. Fromigué, P. J. Marie and A. Lomri, *J Cell Biochem*, 1998, 68, 411-426.
59. M. V. Bais, N. Wigner, M. Young, R. Toholka, D. T. Graves, E. F. Morgan, L. C. Gerstenfeld and T. A. Einhorn, *Bone*, 2009, 45, 254-266.
60. C. S. Soltanoff, S. Yang, W. Chen and Y. P. Li, *Crit Rev Eukaryot Gene Expr*, 2009, 19, 1-46.
61. J. W. Lowery, D. Pazin, G. Intini, S. Kokabu, V. Chappuis, L. P. Capelo and V. Rosen, *Crit Rev Eukaryot Gene Expr*, 2011, 21, 177-185.

View Article Online
DOI: 10.1039/C4TB00837E

62. H. Peng, V. Wright, A. Usas, B. Gearhart, H. C. Shen, J. Cummins and J. Huard, *J Clin Invest*, 2002, 110, 751-759.
63. D. Wotton and J. Massague, *Curr Top Microbiol Immunol*, 2001, 254, 145-164.
64. L. Xiao, Y. Du, Y. Shen, Y. He, H. Zhao and Z. Li, *Frontiers in bioscience : a journal and virtual library*, 2012, 17, 2667-2674.
65. J. M. Norian, M. Malik, C. Y. Parker, D. Joseph, P. C. Leppert, J. H. Segars and W. H. Catherino, *Reprod Sci*, 2009, 16, 1153-1164.
66. A. L. Theiss, J. G. Simmons, C. Jobin and P. K. Lund, *J Biol Chem*, 2005, 280, 36099-36109.
67. D. E. Sullivan, M. Ferris, D. Pociask and A. R. Brody, *Am J Respir Cell Mol Biol*, 2005, 32, 342-349.

View Article Online
DOI: 10.1039/C4TB00837E

Table 1. The ionic concentrations of medium for SZS and HA coatings at different culture conditions.

Medium conditions		Culture medium immersed		Macrophage conditioned		Osteoclast conditioned		Culture time
Coating Materials		SZS	HA	SZS	HA	SZS	HA	
Ionic Concentration (ppm)	Sr	425.10	0.78	483.24	0.51	457.32	0.48	3 day
	Si	58.86	1.26	61.62	1.29	55.86	1.23	
	Zn	39.66	0	44.97	0	43.62	0	
	Ca	43.05	60.57	43.89	89.67	43.95	80.43	
	Sr	390.39	0.99	408.15	0.75	365.88	0.63	6 day
	Si	58.53	0.66	59.43	0.54	54.72	0.45	
	Zn	39.39	0	42.99	0	40.41	0	
	Ca	48.96	53.25	48.81	75.33	47.91	74.79	

View Article Online
DOI: 10.1039/C4TB00837E

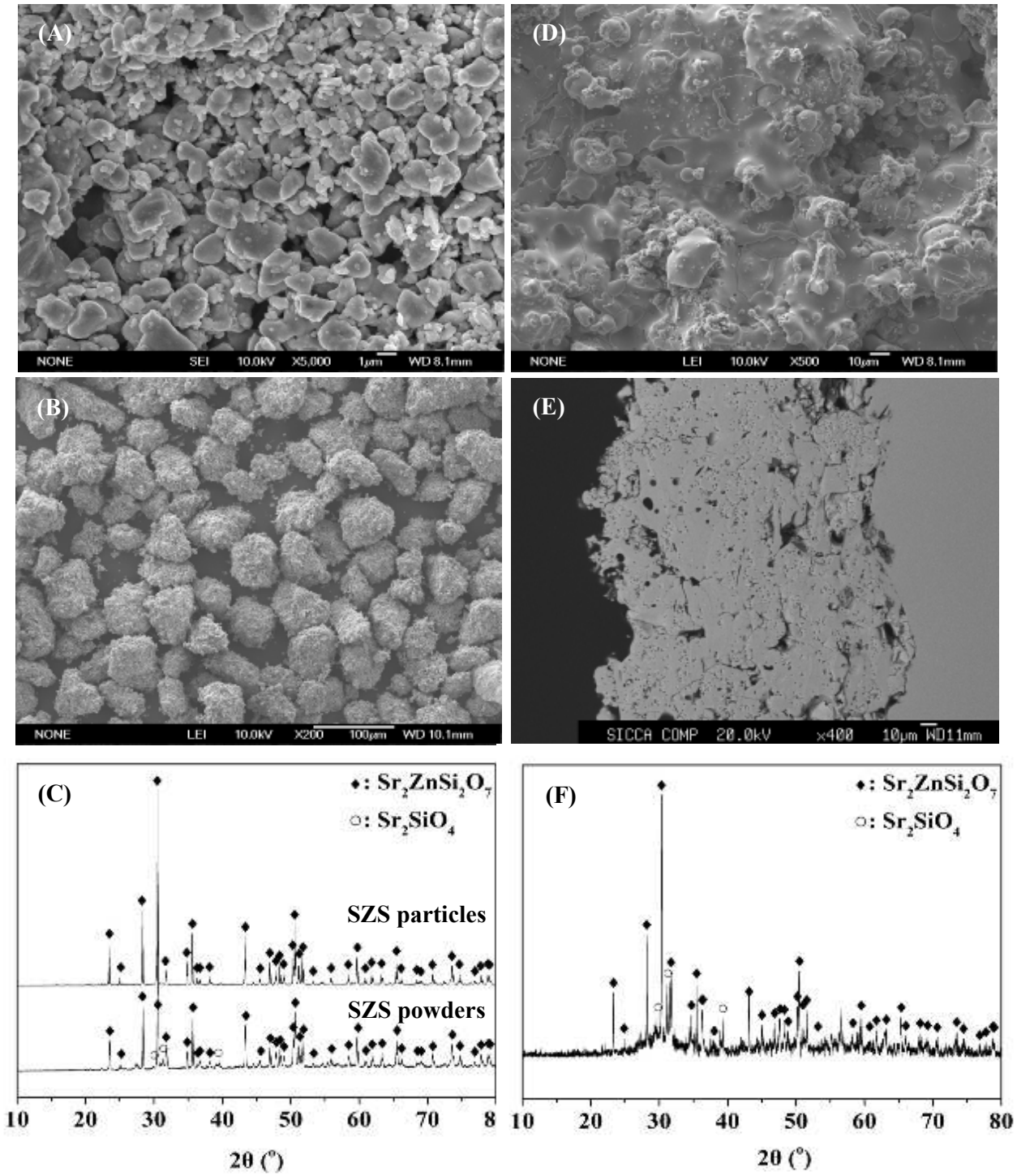

Figure 1. (A) SEM of the solid-reaction synthesized SZS powders; (B) Reconstituted SZS particles prepared by sinter-crushing method; (C) XRD of the SZS powders and particles; (D) and (E) SEM of the surface and cross sections of SZS coatings on the Ti-6Al-4V substrate; (F) XRD of the prepared SZS coatings.

View Article Online
DOI: 10.1039/C4TB00837E

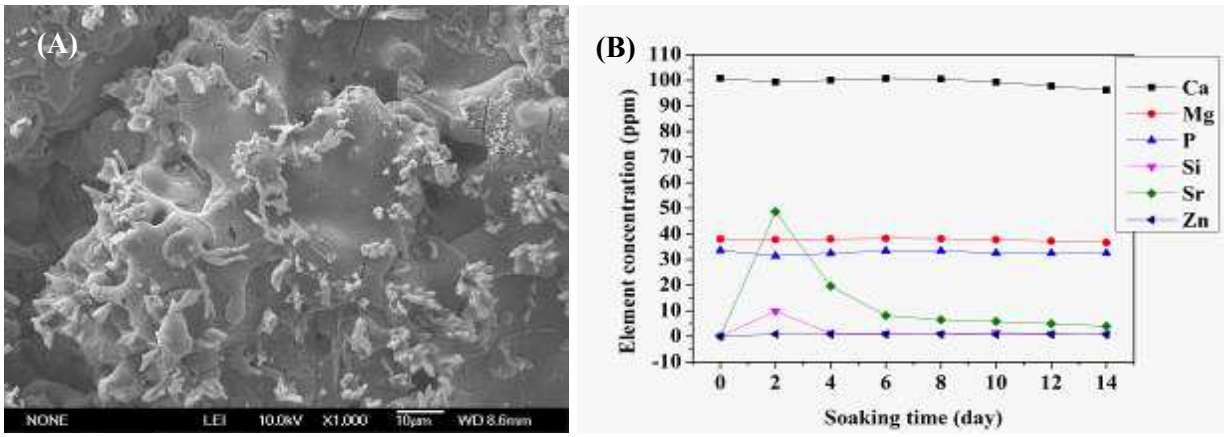

Figure 2. (A) SEM of the surface of SZS coatings after soaking in phosphate-buffered solution; (B) Ionic concentration changes in the solution suggest that the prepared SZS coatings have high chemical stability with low dissolution.

View Article Online
DOI: 10.1039/C4TB00837E

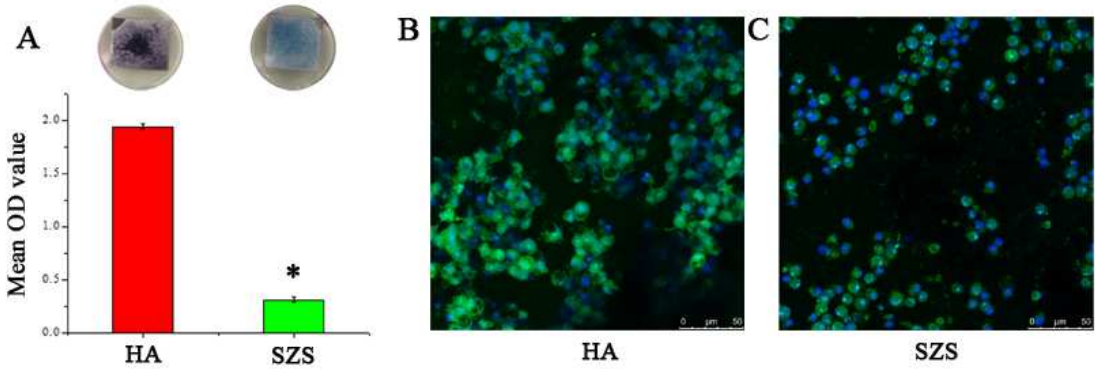

Figure 3. (A). MTT showing the overall metabolic activity of RAW 264.7 cells after 1 day cultured on the suface of coated Ti-6Al-4V. *: Significant difference ($P<0.05$) of SZS group compared with HA group. (B) (C). RAW 264.7 cells after 1 daycultured on the suface of coated Ti-6Al-4V, showing the nuclei and cytoskeleton stained by DAPI and phalloidin with FITC respectively.

View Article Online
DOI: 10.1039/C4TB00837E

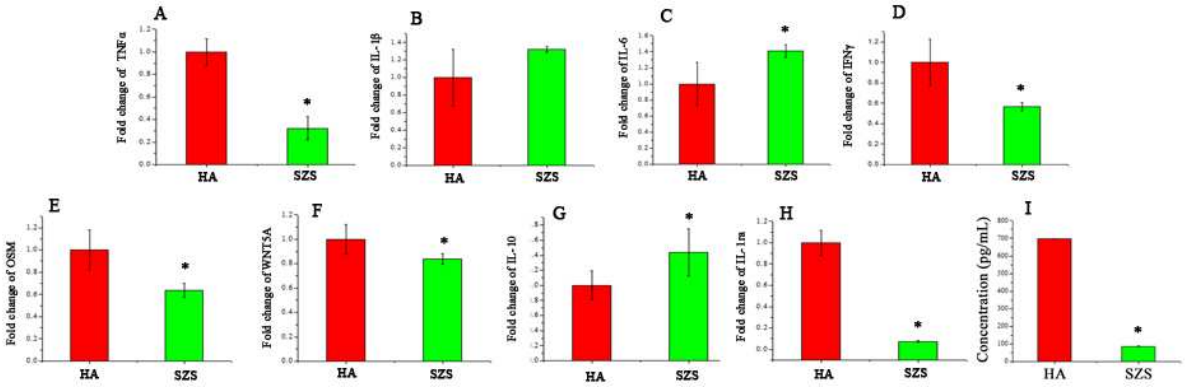

Figure 4. Fold changes of inflammation related genes (A). *TNFα*, (B). *IL1β*, (C). *IL6*, (D). *IFNγ*, (E). *OSM*, (F). *WNT5A*, (G). *IL10* and (H). *IL1ra* in RAW 264.7 cells cultured on the coated Ti-6Al-4V. (I). TNFα secretion from RAW 264.7 cells cultured on the coated Ti-6Al-4V detected by ELISA. *: Significant difference ($P<0.05$). TNFα, IL1β, IL6, IFNγ, and OSM are pro-inflammatory cytokines. WNT5A is an indicator of inflammatory response. IL10 and IL1ra are anti-inflammatory cytokines.

View Article Online
DOI: 10.1039/C4TB00837E

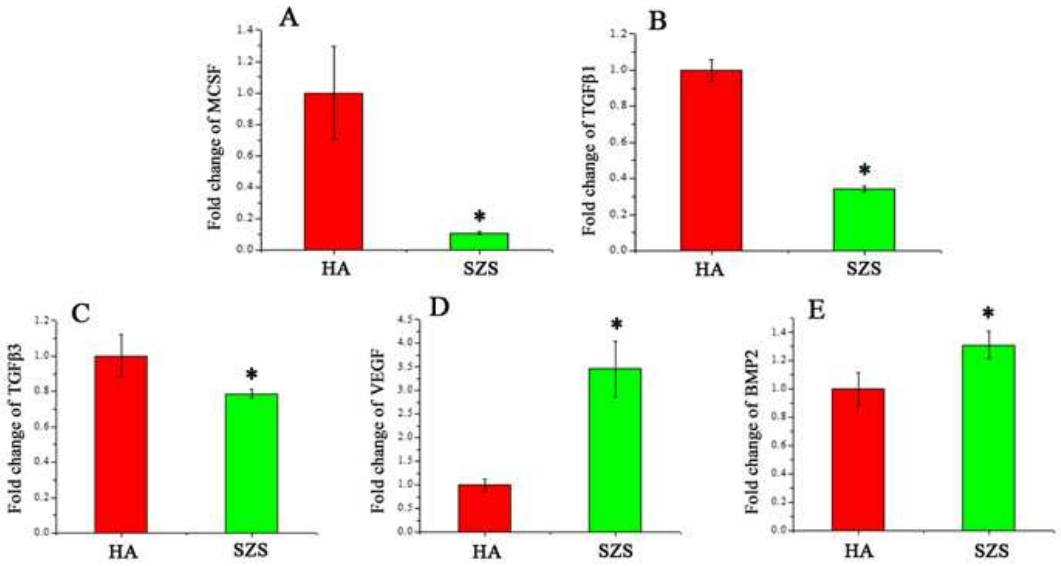

Figure 5. Fold changes of osteogenesis related genes: (A). *MCSF*, (B). *TGFβ1*, (C). *TGFβ3*, (D). *VEGF*, (E). *BMP2* in RAW 264.7 cells cultured on the coated Ti-6Al-4V. *: Significant difference ($P<0.05$). MCSF is an osteoclastogenic cytokines. TGFβ1 and TGFβ3 are profibrotic factors. VEGF is an angiogenic and vasculogenic factor. BMP2 is an osteogenic factor.

View Article Online
DOI: 10.1039/C4TB00837E

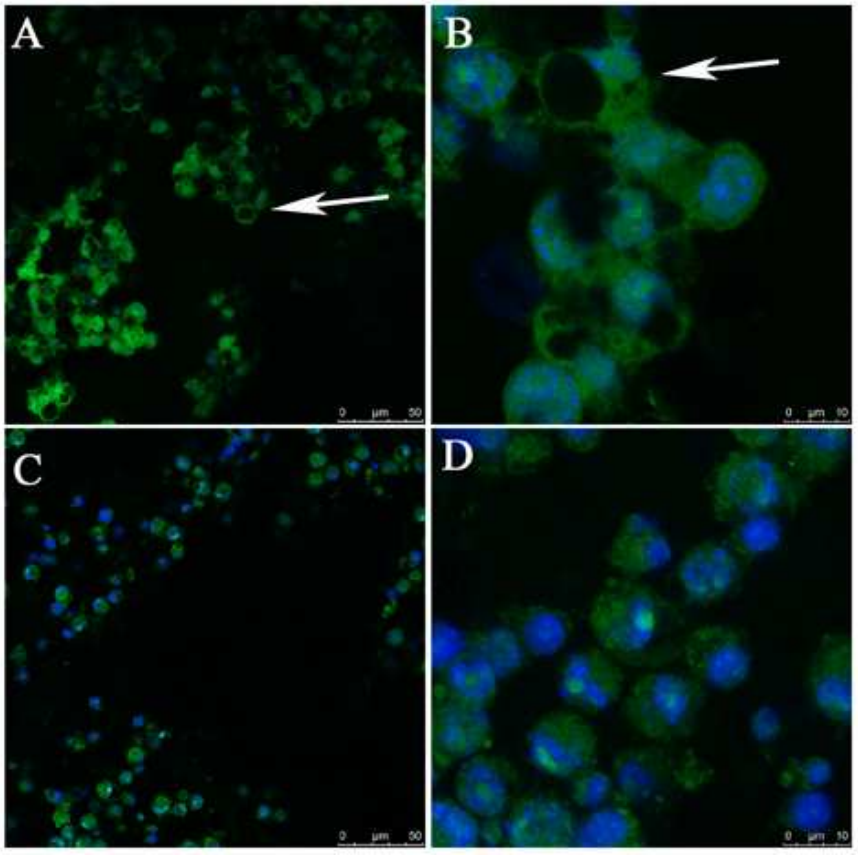

Figure 6. Phagocytosis of the coating materials. RAW 264.7 cells were stained by DAPI and phalloidin with FITC for the nuclei and cytoskeleton respectively. (A) (B). HA: RAW 264.7 cells internalized the HA particles, forming a big "bubble" within the cytoplasma, which was observed in the majority of the stimulated cells; (C) (D). SZS: this feature was rarely observed in the SZS coating stimulating RAW 264.7 cells.

View Article Online
DOI: 10.1039/C4TB00837E

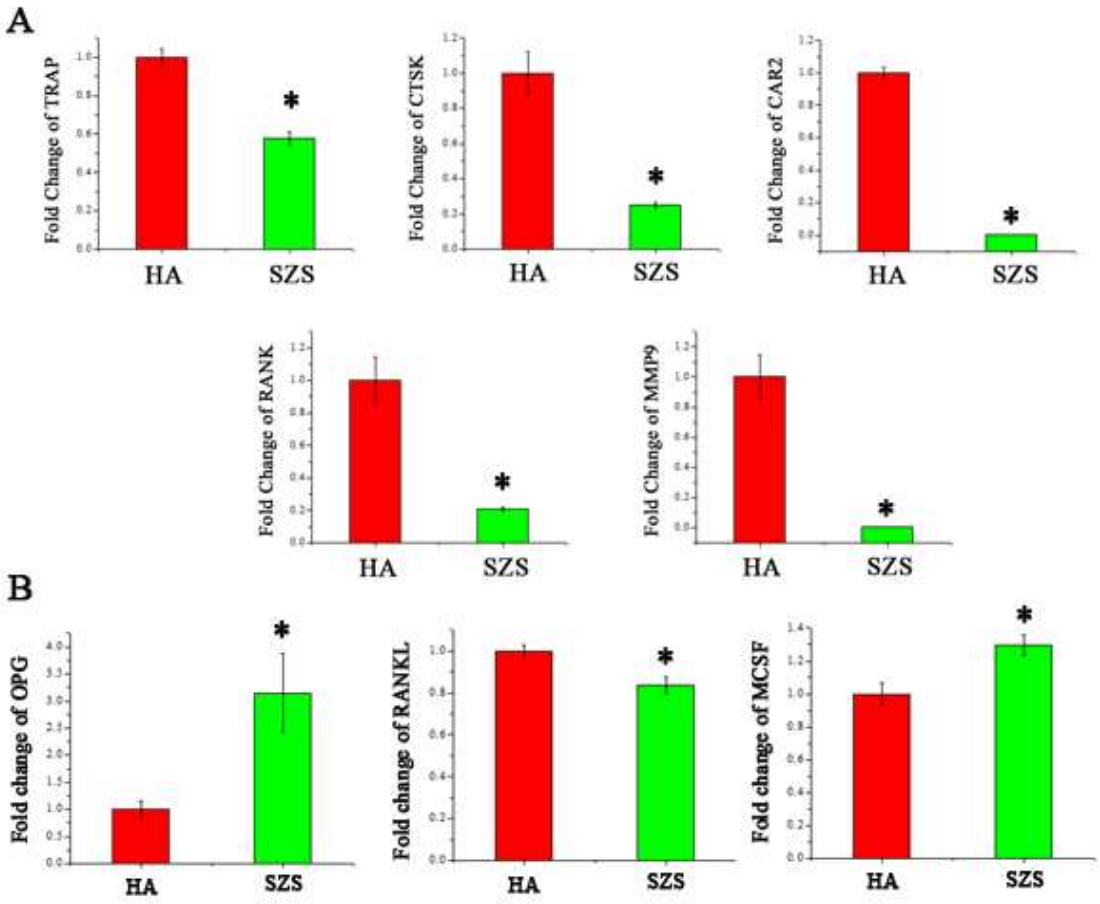

Figure 7. (A). Fold changes of osteoclast activities related genes: *TRAP*, *CTSK*, *CA2*, *RANK* and *MMP9* in RAW 264.7 cells cultured on the coated Ti-6Al-4V. The upregulation of *TRAP*, *CTSK*, *CA2*, *RANK* and *MMP9* indicates higher osteoclast activities. (B). Fold changes of osteoclastogenesis related genes: *OPG*, *RANKL*, and *MCSF* by BMSCs stimulated by the conditioned medium. *: Significant difference ($P<0.05$). RANKL and MCSF are osteoclastogenic cytokines. OPG is a decoy receptor of RANKL, interrupting the binding of RANKL with RANK receptor, thereby inhibiting osteoclastogenesis.

View Article Online
DOI: 10.1039/C4TB00837E

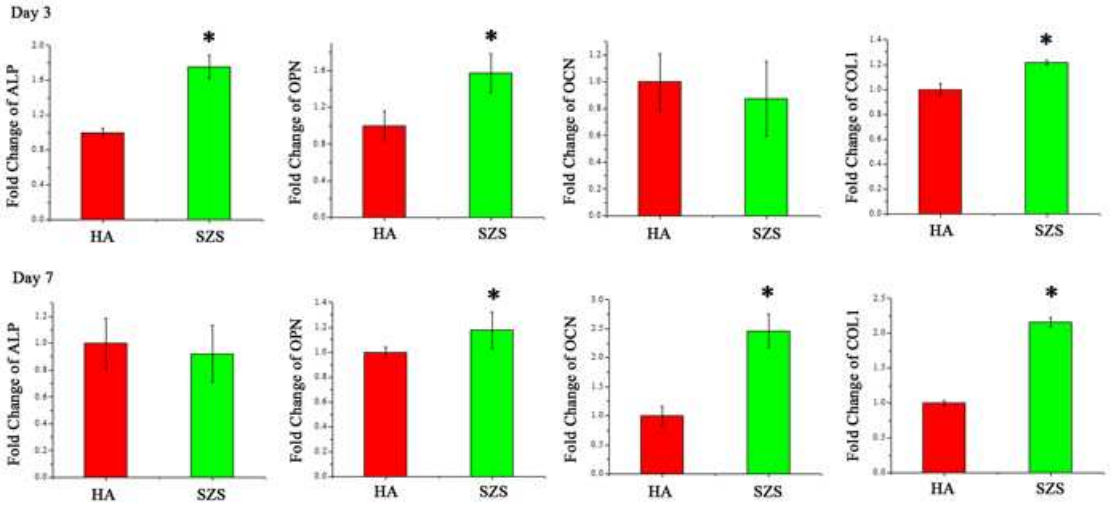

Figure 8. Osteogenesis related gene expression (*ALP*, *OPN*, *OCN*, *COL1*) by BMSCs stimulated by the conditioned medium in day 3 and 7. *: Significant difference ($P<0.05$). The upregulation of *ALP*, *OPN*, *OCN* and *COL1* indicates better osteogenesis.

View Article Online
DOI: 10.1039/C4TB00837E

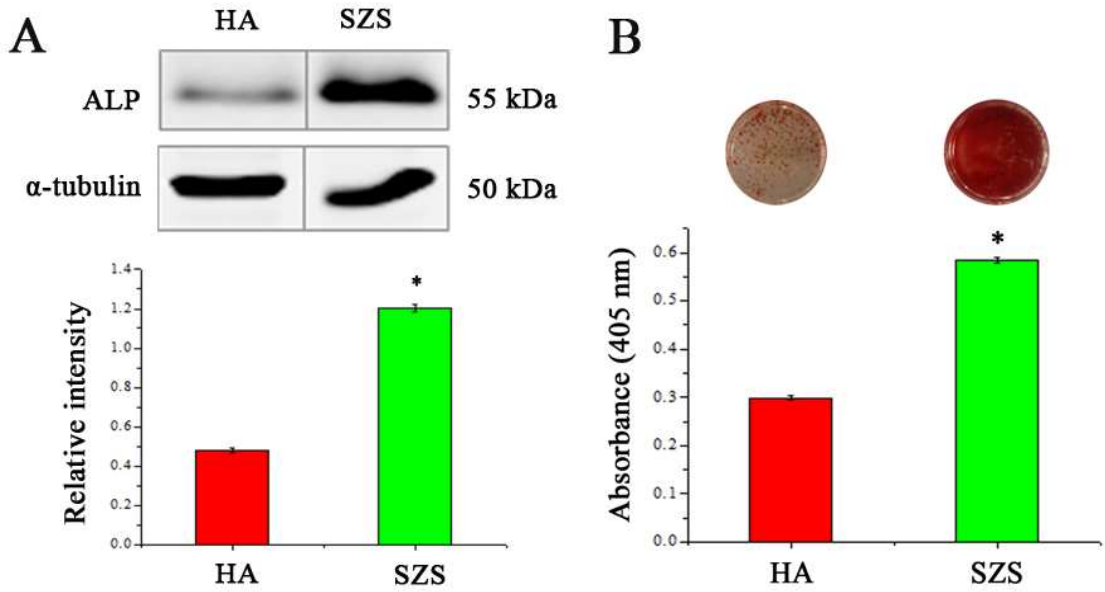

Figure 9. (A). Western blot analysis of ALP expression by BMSCs stimulated by the conditioned medium. (B). Alizarin Red S staining of BMSCs stimulated by the conditioned medium with osteogenic supplements. *: Significant difference ($P<0.05$).

View Article Online
DOI: 10.1039/C4TB00837E

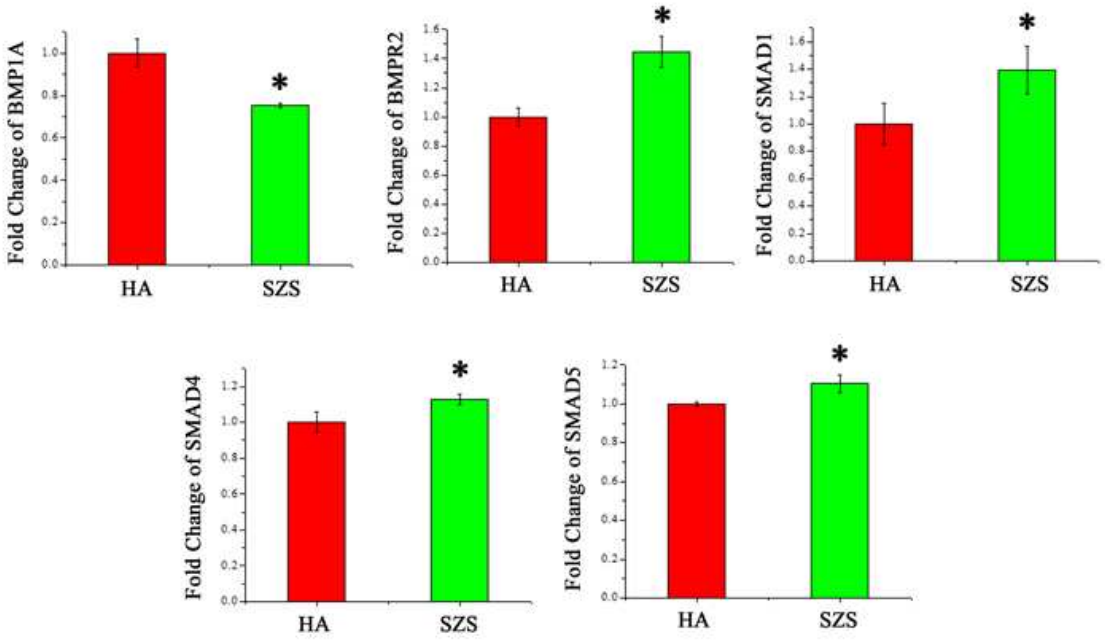

Figure 10. Fold changes of BMP2 signalling pathway genes *BMPR1A*, *BMPR2*, *SMAD1*, *SMAD5* and *SMAD4* in BMSCs stimulated by the conditioned medium. *: Significant difference ($P<0.05$). The upregulations of *BMPR1A*, *BMPR2*, *SMAD1*, *SMAD5* and *SMAD4* indicate the activation of BMP2 signalling pathway.

View Article Online
DOI: 10.1039/C4TB00837E

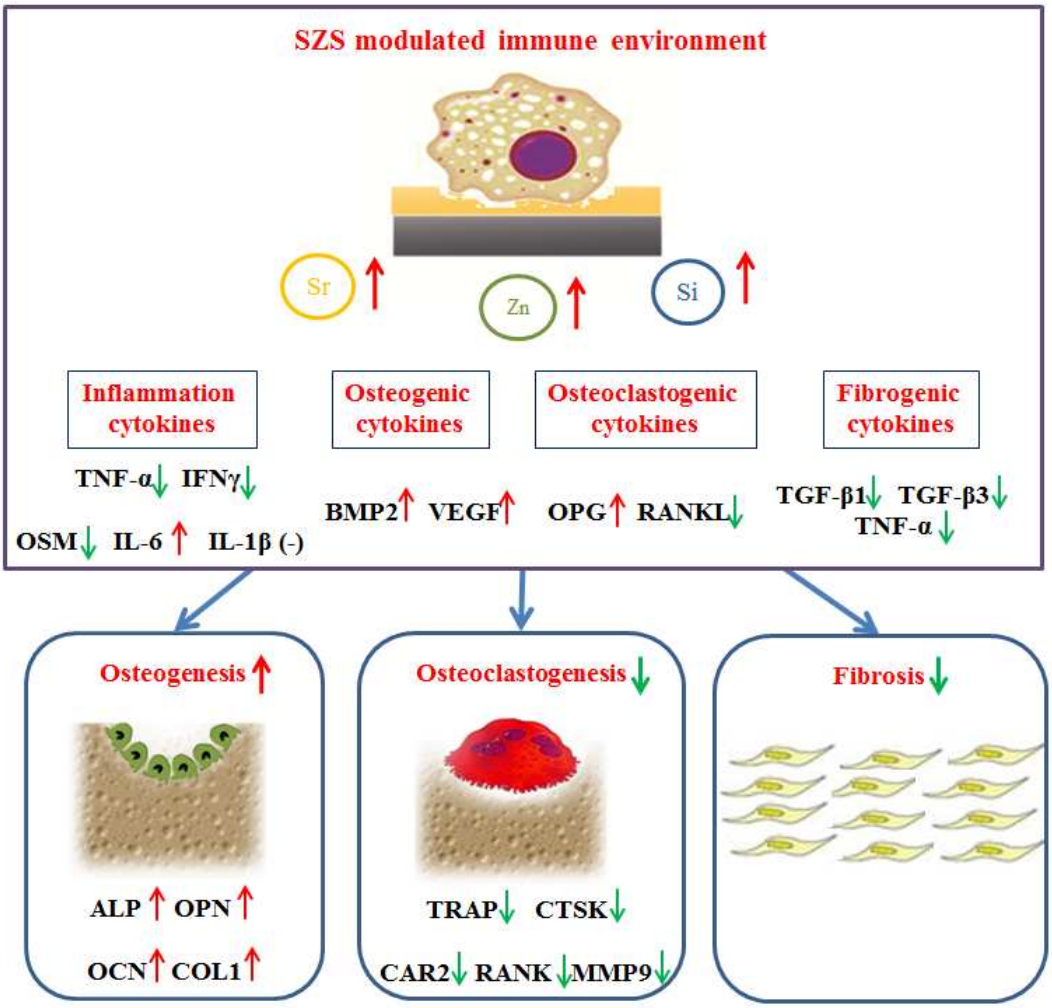

Figure 11: Scheme illustration of the modulatory effects of SZS on immune environment and the subsequent effects on osteogenesis and osteoclastogenesis.

View Article Online
DOI: 10.1039/C4TB00837E

Table of Contents

J Mater Chem B. Nutrient element-based $Sr_2ZnSi_2O_7$ coatings induce favorable osteoimmunomodulation to enhance the osteogenic differentiation.

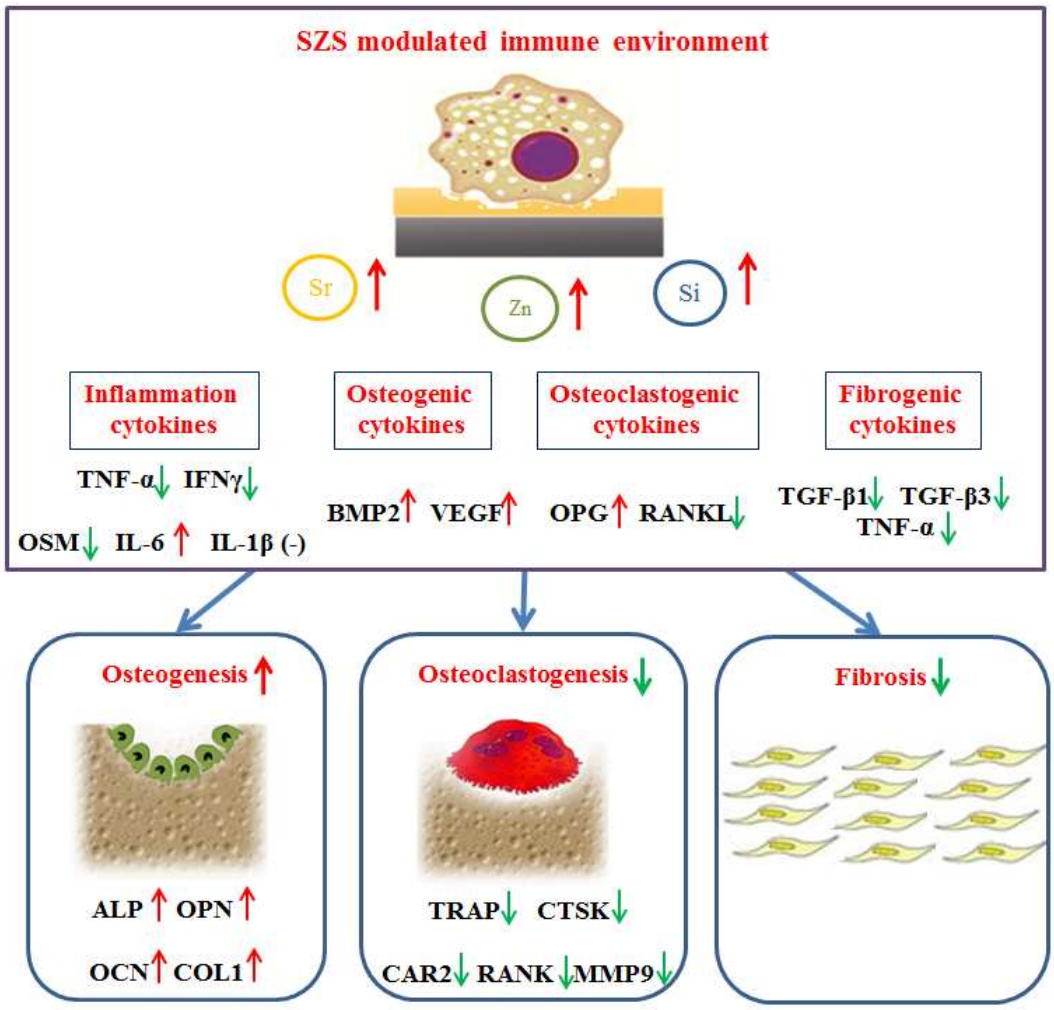

Material chemistry of $Sr_2ZnSi_2O_7$ coating modulates the immune environment to induce osteogenic differentiation of BMSCs by activating BMP2 signalling pathway.